Received: 25 December 2019 | Revised: 16 July 2020 | Accepted: 18 July 2020

DOI: 10.1002/nbm.4389

RESEARCH ARTICLE

NMR IN BIOMEDICINE WILEY

A pilot study of magnetic resonance fingerprinting in Parkinson's disease

Vera Catharina Keil[1,2] | Stilyana Peteva Bakoeva[1,3] | Alina Jurcoane[1,4] | Mariya Doneva[5] | Thomas Amthor[5] | Peter Koken[5] | Burkhard Mädler[6] | Guido Lüchters[7] | Wolfgang Block[8] | Ullrich Wüllner[9,10] | Elke Hattingen[1,4]

[1]Department of Neuroradiology, University Hospital Bonn, Bonn, Germany

[2]Department of Radiology, Amsterdam University Medical Center, Amsterdam, the Netherlands

[3]Department of Neurology, University Hospital Duesseldorf, Düsseldorf, Germany

[4]Institute for Neuroradiology, University Hospital, Goethe University Frankfurt am Main, Frankfurt, Germany

[5]Philips Research, Hamburg, Germany

[6]Philips GmbH, UB Healthcare, Hamburg, Germany

[7]Zentrum für Entwicklungsforschung, University of Bonn, Bonn, Germany

[8]Department of Radiology, University Hospital Bonn, Bonn, Germany

[9]Department of Neurology, University Hospital Bonn, Bonn, Germany

[10]Deutsches Zentrum für Neurodegenerative Erkrankungen (DZNE), Bonn, Germany

Correspondence
Vera Catharina Keil, Department of Neuroradiology, University Hospital Bonn, Venusberg Campus 1, 53127, Bonn, Germany.
Email: vera.keil@ukbonn.de

Parkinson's disease (PD) affects more than six million people, but reliable MRI biomarkers with which to diagnose patients have not been established. Magnetic resonance fingerprinting (MRF) is a recent quantitative technique that can provide relaxometric maps from a single sequence. The purpose of this study is to assess the potential of MRF to identify PD in patients and their disease severity, as well as to evaluate comfort during MRF. Twenty-five PD patients and 25 matching controls underwent 3 T MRI, including an axial 2D spoiled gradient echo MRF sequence. T1 and T2 maps were generated by voxel-wise matching the measured MRF signal to a precomputed dictionary. All participants also received standard inversion recovery T1 and multi-echo T2 mapping. An ROI-based analysis of relaxation times was performed. Differences between patients and controls as well as techniques were determined by logistic regression, Spearman correlation and t-test. Patients were asked to estimate the subjective comfort of the MRF sequence. Both MRF-based T1 and T2 mapping discriminated patients from controls: T1 relaxation times differed most in cortical grey matter (PD 1337 ± 38 vs. control 1386 ± 37 ms; mean ± SD; P = .0001) and, in combination with normal-appearing white matter, enabled correct discrimination in 85.7% of cases (sensitivity 83.3%; specificity 88.0%; receiver-operating characteristic [ROC]) area under the curve [AUC] 0.87), while for T2 mapping the left putamen was the strongest classifier (40.54 ± 6.28 vs. 34.17 ± 4.96 ms; P = .0001), enabling differentiation of groups in 84.0% of all cases (sensitivity 80.0%; specificity 88.0%; ROC AUC 0.87). Relaxation time differences were not associated with disease severity. Standard mapping techniques generated significantly different relaxation time values and identified other structures as different between groups other than MRF. Twenty-three out of 25 PD patients preferred the MRF examination instead of a standard MRI. MRF-based mapping can identify PD patients with good comfort but

Abbreviations used: BCa, bias-corrected accelerated; CI, confidence intervals; EPG, extended phase graphs; GM, grey matter; H&Y, Hoehn and Yahr scale; MAH, more affected hemisphere; MMSE, Minimal-Mental State Examination; MRF, MR fingerprinting; NAWM, normal-appearing white matter; PD, Parkinson's disease; UPDRS, Unified Parkinson's Disease Rating Scale; WM, white matter.

needs further assessment regarding disease severity identification and its potential for comparability with standard mapping technique results.

KEYWORDS
MR fingerprinting, Parkinson's disease, relaxometry, T1 mapping, T2 mapping

1 | INTRODUCTION

Parkinson's disease (PD) has an estimated prevalence of more than 6 million worldwide, affecting ~ 1% of those aged older than 65 years. It is considered the second most frequent neurodegenerative disease, and its incidence is rising in comparison with other neurodegenerative diseases.[1]

While PD is a clinical diagnosis sui generis—with clinical disease severity assessment based on either the Unified Parkinson's Disease Rating Scale (UPDRS)[2] or the Hoehn and Yahr scale (H&Y),[3] and clinical diagnosis being established using national examination guidelines—the majority of patients with suspected PD receive two imaging-based examinations of the brain as part of the diagnostic process: MRI to exclude structural pathologies and a dopamine transporter single-photon emission computed tomography (or DATSPECT, the 23Ioflupane DaTSCAN). The latter has a high sensitivity with which to confirm the loss of striatal dopamine transporters, and therefore PD, but it is expensive, carries a radiation burden and, consequently, is not adequate for regular monitoring.[4] On the other hand, more accessible visual MRI biomarkers of PD, such as the swallow-tail sign, are neither quantitative nor totally reliable.[2,5]

T1, T2 and T2* relaxometric MRI studies identified PD-specific changes attributed to alterations in the biochemistry and connectome of patients.[6–8] For example, iron accumulation and changes in the brain perfusion of PD patients leads to alterations in T1 and T2 relaxation times compared with people without PD.[7,9] Quantitative parameters with cut-off values could be established to separate non-PD people from those with PD or associated pathologies. The first mapping studies already pointed in this direction.[6,7]

Magnetic resonance fingerprinting (MRF) is a more recent quantitative MRI technique allowing the generation of T1 and T2 maps as well as synthetic weightings without the application of external agents from a single sequence.[10] Allowing the reconstruction of many standard types of weighting as well as quantitative maps, MRF has the potential to significantly shorten examination times. This can reduce pain and distress in the multi-morbid group of mainly elderly patients. MRF applies pseudo-random variations of flip angles, repetition times and k-space sampling to yield a unique signal evolution for each voxel that acts as a "fingerprint" for the corresponding tissue. The dictionary used to identify the fingerprint is based on simulated signal evolutions, including the range of the expected relaxation time values. MRF has already demonstrated its clinical usefulness regarding glioma diagnostics and brain ageing.[11,12]

This is a cross-sectional pilot study to explore the potential of MRF in the mapping-based identification of PD with further regard to correlation with disease severity. Findings are compared with those gained by established T1 and T2 mapping techniques. This study also includes a brief assessment of patient comfort during MRF scanning procedures.

2 | EXPERIMENTAL

2.1 | Study overview

Although this is a cross-sectional study, longer disease duration was assumed to be correlated to a higher UPDRS. Recruitment for this prospective, institutional review board ethics-approved, single-centre study, took place from February 2018 to February 2019 after written informed consent had been received from all participants. All PD patients (n = 25) had received their diagnosis at least 1 year prior to study inclusion and had undergone previous MRI. Twenty-five non-PD sex- and age-balanced volunteering controls received the same MRI protocol as the PD patients. The protocol involved an MRF sequence to generate T1 and T2 maps and sequences for standard technique T1 and T2 mapping (standard T1 and T2 mapping from hereon). Regional T1 and T2 relaxation times between patients and controls were also compared between techniques. We analysed ROI-based brain structure volumes, and clinical correlations with relaxation times. Patients were also surveyed regarding the general comfort of the MRF sequence. A workflow summary is presented in Figure 1.

2.2 | Clinical assessment and recruitment criteria

PD patients and controls had to be aged 18 years or older and also legally allowed to give informed consent. Participants had to answer a concise health questionnaire prior to MRI regarding cardiovascular risk factors, diabetes, smoking and other neurological conditions, including psychiatric

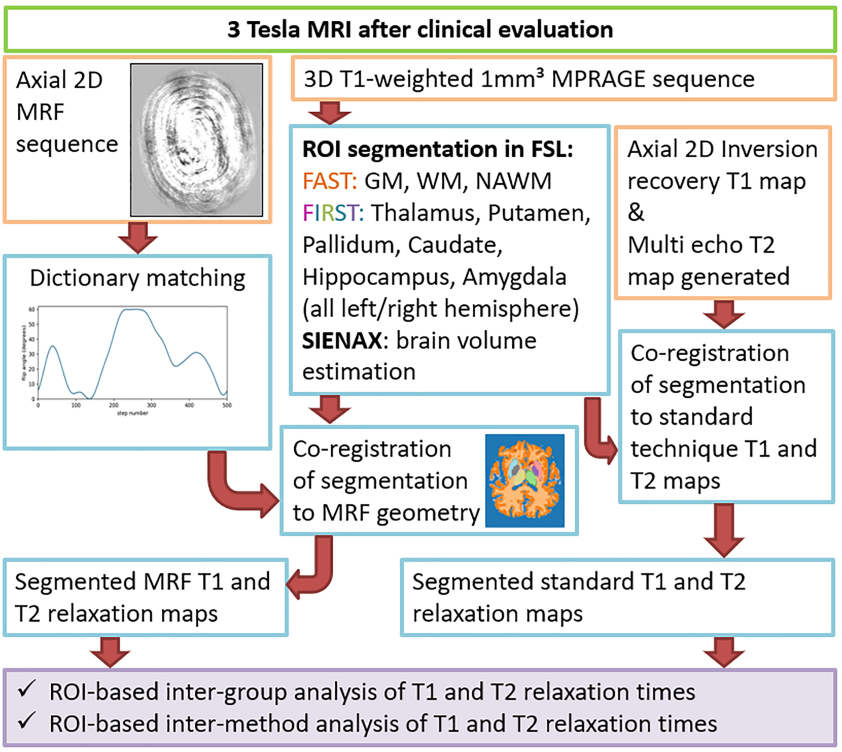

FIGURE 1 Overview of the magnetic resonance fingerprinting (MRF) image acquisition and processing. FAST and FIRST: programs in FSL software; GM, cortical grey matter; MPRAGE, magnetisation-prepared rapid gradient echo; NAWM, normal-appearing white matter; ROI, region of interest; SIENAX, SIENA (Structural Image Evaluation using Normalisation of Atrophy X); WM, all white matter

diseases and intoxications. Controls were not allowed to show clinical signs of PD, as defined by our national guidelines, upon examination.[13] In both groups, hypertension under treatment was accepted, provided no hypertensive crisis had occurred that needed any form of acute treatment in the past year. A history of smoking was allowed if the participant had stopped smoking at least 1 year before MRI. The exclusion criteria for both groups consisted of diagnosed diabetes, obesity (body mass index > 30 kg/m^2), a history of resuscitation, stroke, severe head trauma, brain tumour or meningitis, any form of active cancer treatment or suspected neurological disease affecting the central nervous system. PD diagnosis was the only neurological diagnosis allowed in the PD group, and it had to have been confirmed following the 2015 Movement Disorder Society criteria before study inclusion.[14] Tremor-dominant PD patients were excluded due to concerns regarding motion artefacts. A wide variety of duration of symptoms and variable medication regimens were accepted. All PD patients needed to be responsive to levodopa and had a previous DATScan confirming clinically suspected PD at some point before the study. Other conditions of the PD spectrum, such as (suspected) multisystem atrophy type P or dementia in PD, were exclusion criteria. Contraindications for 3 T MRI were exclusion criteria. UPDRS, H&Y and Minimal-Mental State Examination (MMSE) tests were performed on the day of MRI during an on-phase of medication. An MMSE result of >26/30 points was accepted for controls. By comparison, PD patients were allowed to participate at 26 points, as mild cognitive deficit without dominant forms of dementia is common.[14] PD symptoms are regularly asymmetric, and the more symptomatic body side was registered. PD patients and controls were excluded after the MRI scan if a pathology other than PD was identified, for example, brain atrophy above age-accepted norms (eg, a global cortical atrophy score of >1 or a mesiotemporal atrophy score of >1 in patients aged <75 years), or any findings which indicated suspicions of stroke or tumour.[15]

2.3 | MRI protocol

All participants were examined at 3 T MRI (Achieva TX, Philips Healthcare, Best, the Netherlands) using an eight-channel head coil. The protocol consisted of a T1-weighted 3D turbo field echo sequence (TR/TE 7.8/3.6 ms; FOV 256 x 256 x 130 mm; voxel size 1 mm^3, 170 slices; acquisition time of 4 minutes 26 seconds), a 3D turbo field echo employing an adiabatic inversion prepulse (inversion recovery [IR]-based T1 mapping sequence) (TR 5.0 ms, TE 2.55 ms, FA 15°, five inversion time delays of 150, 350, 750, 1200 and 2300 ms, FOV 240 × 220 x 70 mm, 28 slices, acquisition time of 5 minutes 0 seconds), a multi-echo–based T2 mapping sequence (TR 1 second, TE 15, 30, 45, 60, 75, 90, 105 and 120 ms, FOV 240 x 212 x 66 mm, 12 slices, acquisition time of 5 minutes 32 seconds) and an axial 2D MRF sequence (TR/TE 15/3.5 ms, FOV 240 x 240 x 60 mm, voxel size 1 x 1 x 5 mm, 12 slices, gap of 0 mm, acquisition time of 3 minutes 12 seconds, two spiral interleaves/slice, acquisition window of 7.0 ms, acceleration factor 15). The MRF sequence covered the temporal and limbic lobes, insula, deep grey matter (GM) structures and the majority of frontal, parietal and occipital lobes. The spoiled gradient echo MRF sequence started with an adiabatic inversion pulse followed by an optimised flip angle sequence (0 to 60°) with read-outs over 500 time-points.[16,17]

2.4 | T1 and T2 relaxation map reconstruction and structural analyses

IR-based T1 maps were generated using MATLAB scripted in-house software, as described elsewhere.[18] Multi-echo T2 maps were automatically created by scanner-integrated software. MRF-based map reconstruction and ROI-based analyses have been described in detail elsewhere.[19] Briefly, dictionary-based MRF reconstruction used the extended phase graphs (EPG) algorithm. T1 was sampled in 10-ms steps between 10 and 2000 ms, T2 was sampled in 1-ms steps between 10 and 200 ms, and in 10-ms steps between 210 and 600 ms. MRF-based T1 and T2 relaxometric maps were originated from inner product pattern matching to identify the best matching "fingerprint"/signal from the dictionary.[20]

Segmentation of 3D structural data and coregistration of the relaxation maps to extract relaxation times were achieved with FSL 5.0 (Oxford, UK) in the 1 mm 3D T1 map space and were then resampled to the 5 mm space of the MRF maps by nearest neighbour interpolation. The following ROIs were segmented: cortical GM, normal-appearing white matter (NAWM), hippocampus, amygdala, putamen, pallidum and caudate. Volumetric analyses of all ROIs were automatically produced in the segmentation process. To normalise volumes to subjects' head size, that is, to make the structure volumes comparable, FSL SIENAX was applied for cortical GM and WM. The resulting scaling factor was ultimately used to determine normalised volumes for deep GM structures.[21,22] ITK-SNAP 3.6.0 was used for visualisation, control of segmentation quality and segmental parameter extraction.[23]

2.5 | Patient comfort rating

Patients were asked to rate the MRF sequence directly after the acquisition and before standard mapping sequence acquisition as either (1) unpleasant, (2) indifferent or (3) comfortable to undergo. Further, they were asked whether they would feel comfortable (1) to opt for the MRF protocol or (2) for the usual hospital MR protocol for neurodegenerative disease follow-up, which was known to them from previous examinations. To guarantee an informed decision, patients received information about the potential benefits of MRF (an increase in comfort through saved time for the patient; potential new ways of data interpretation) versus potential trade-offs (the sequence not being well established; artificial weightings could compromise the diagnostic quality) before entering the scan room during the enrolment procedure.

2.6 | Statistics

A statistician performed all analyses with Stata 14.0. Demographics were analysed by independent sample t-test and Fisher exact tests, respectively, after positive Shapiro-Walk testing for Gaussian distribution of values.

Normally distributed relaxometric values and regional volumetric measurements were compared with t-tests, and the Benjamini-Hochberg procedure corrected for false discovery.[24] Bootstrapping with 2000 samples using a random seed was used to assess result robustness and bias-corrected accelerated (BCa) confidence intervals (CI). Additional Cohen's D effect size calculations were performed for significantly differing structures. A Cohen's D of at least 0.80 was considered a large effect; from 0.5 a medium effect was assumed. Relaxation time differences between PD patients and controls were analysed with stepwise regression. To avoid overfitting, the analysis was conservatively limited to a maximum of two relevant variables as contributing factors.[25,26] These were further explored with sensitivity/specificity as well as receiver-operating characteristic (ROC) analyses stating the positive likelihood ratio, LR+. To account for a potential asymmetry of symptoms statistics were performed twice: once for ROIs defined by hemisphere (eg, the structure of a PD patient's left hemisphere compared with the structure of a control's left hemisphere), and second, with ROIs classified by the hemisphere contralateral to the clinically more affected body side. Standard mapping technique and MRF-based relaxation times were compared with paired t-tests and with Spearman Rho rank test. Disease duration and severity of disease were correlated to T1 and T2 relaxation times with Spearman Rho rank test. A subgroup analysis of patients with recent symptom onset versus longstanding onset was performed with paired and unpaired t-tests.

3 | RESULTS

3.1 | Participant demographics

Two of the initial 27 patients and three of the initial 28 volunteer controls were excluded due to secondary brain pathology identified during the MRI study (n = 2 poststroke defects, n = 1 pathological atrophy, n = 1 normal-pressure hydrocephalus stigmata, n = 1 haemorrhage residuals), leaving 25 patients and 25 controls. The 25 remaining patients (eight women, 17 men) had a mean age of 68.72 ± 7.0 (range 63-80) years and the mean MMSE was 29.04 ± 1.77 (range 26-30) points. Controls (n = 25; 10 women, 15 men; MMSE 29.48 ± 0.82 [range 28-30] points; age 68.8 ± 4.93 [range 51-78] years) and patients did not differ significantly in age (P = .963), MMSE (P = .265) or sex distribution (P = .565).

Seventeen patients showed a right body side-dominant PD (assuming a more affected left hemisphere); the others were left body side-dominant. Mean UPDRS was 44.08 ± 23.53 (range 9-104) points, mean H&Y was 3.10 ± 0.58 (range 2-4) points and mean time between the initial diagnosis of PD and study participation was 7.96 ± 5.14 (range 2-18) years.

3.2 | MRF-based mapping in patients and controls

With a regression coefficient R^2 of 0.33, regression analysis identified cortical GM (OR 0.955; P = .0001) and NAWM (OR 1.017; P = .035) as the two most relevant structures with which to separate PD patients from controls when using MRF-based T1 mapping. Based on these classifiers, a correct separation between both groups was achievable in 85.71% of cases (sensitivity 83.33%; specificity 88.0%; LR+ 6.94; cut-off point 0.5022). The positive predictive value (PPV) was 86.96%, while the negative predictive value (NPV) was 84.62%. ROC analysis rendered an area under the curve (AUC) of 0.87 (95% CI 0.768-0.978; Figure 2).

The margins probability analysis revealed an ideal cut-off relaxation time at 1350 ms in cortical GM. GM T1 relaxation times were significantly shorter in patients compared with controls (P = .0001; Cohen's D = 1.29, CI of D 0.72-1.86; Figure 3A; Table 1). Further structures with significant, false discovery-corrected differences in T1 relaxation times were the left caudate (P = .025; Cohen's D = 0.71, CI of D 0.14-1.28), both hippocampi (both P = .028; Cohen's D left hippocampus = 0.56, CI of D 0-1.12; Cohen's D right hippocampus = 0.75, CI of D 0.18-1.32) and amygdalae (P = .020 left; Cohen's D = 0.86, CI of D 0.29-1.43; P = .025 right; Cohen's D = 0.78, CI of D 0.21-1.35; Figure 3A). In summary, PD patients showed consistently shorter T1 relaxation times than controls in several brain structures, albeit in the range of 2.84%-4.40% less than controls (Table 1). Differences in the left hippocampus were the only ones to lose significance after bootstrapping (P = .053).

In MRF-based T2 mapping, differences between patients and controls were inversed: T2 relaxation times were consistently longer in patients than in controls (Figure 3B; Table 1). By applying MRF-based T2 mapping, relaxation times in GM (OR = 0.804; P = .005) and the left putamen (OR = 1.70; P = .001) were identified as the most relevant structures with which to separate both groups (R^2 = 0.376). These two classifiers rendered a correct separation in 84.0% of all cases (sensitivity 80.0%; specificity 88.0%; LR+ 6.67; cut-off point 0.5016). The PPV was 86.96%, while the NPV was 81.48%. The ROC analysis showed an AUC of 0.87 (95% CI 0.773-0.973; Figure 4).

Significant T2 relaxation time differences were found in both putamina (P = .001 left, Cohen's D = 1.13, CI of D 0.56-1.69; P = .015 right, Cohen's D = 0.81, CI of D 0.24-1.38; Figure 3B; Table 1) and globus pallidus (P = .015 left, Cohen's D = 0.84, CI of D 0.27-1.41; P = .01 right, Cohen's D = 0.93, CI of D 0.36-1.50) as well as the left thalamus (P = .034, Cohen's D = 0.70, CI of D 0.13-1.27) and left amygdala (P = .040,

FIGURE 2 Receiver-operating characteristic (ROC) area under the curve (AUC) of patient-control separation based on cortical grey matter and normal-appearing white matter T1 relaxation times

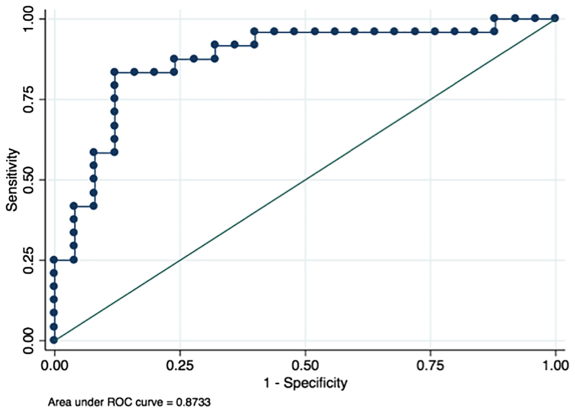

FIGURE 3 Significantly differing T1 and T2 relaxation times of brain structures in nonmultiple testing corrected data. A, T1 relaxation times; B, T2 relaxation times. Graph illustrates mean and standard deviation in 25 subjects per group. Normal-appearing white matter (NAWM) was no longer significantly differing as a ROI after Benjamini-Hochberg correction (P = .070; compare with Table 1). GM, grey matter; PD, Parkinson's disease. P-values: * < .05; ** < .01; *** < .001

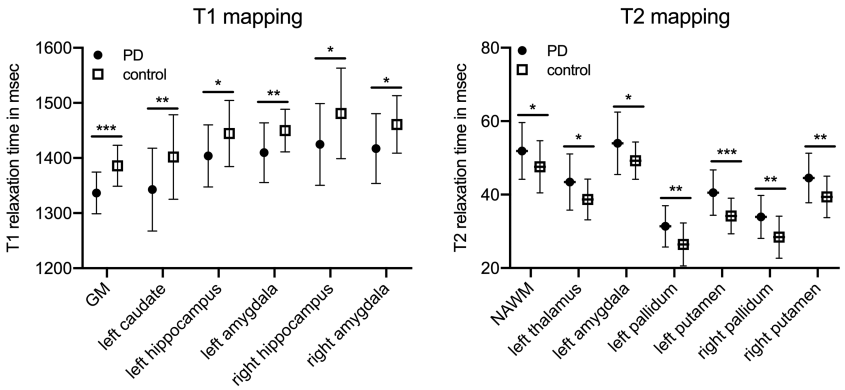

TABLE 1 Relative and absolute differences of relaxation times in region of interest (ROI) structures with significant differences between patients (n = 25) and controls (n = 25)

ROI structure	percentage difference PD vs. control	uncorrected P-value	Benjamini-Hochberg adjusted P-value	group	relaxation time (ms)
MRF-based mapping					
T1 mapping					
GM	3.69%	.0001	**.0001**	**patient**	1340.36 ± 33.43
				control	1385.97 ± 37.21
left caudate	4.40%	.008	**.025**	**patient**	1342.77 ± 75.14
				control	1401.80 ± 76.78
left hippocampus	2.89%	.017	**.028**	**patient**	1403.97 ± 56.34
				control	1444.53 ± 59.98
left amygdala	2.84%	.004	**.020**	**patient**	1409.67 ± 54.04
				control	1449.83 ± 38.64
right hippocampus	3.95%	.014	**.028**	**patient**	1424.73 ± 74.12
				control	1480.94 ± 82.14
right amygdala	3.09%	.010	**.025**	**patient**	1417.26 ± 63.33
				control	1460.98 ± 52.14
T2 mapping					
NAWM	9.09%	.049	.070	**patient**	51.89 ± 7.56
				control	47.56 ± 7.26
left thalamus	12.32%	.017	**.034**	**patient**	43.44 ± 7.82
				control	38.67 ± 5.66
left amygdala	9.60%	.024	**.040**	**patient**	53.97 ± 8.66
				control	49.24 ± 5.19
left pallidum	18.64%	.005	**.015**	**patient**	31.35 ± 5.72
				control	26.42 ± 5.97
left putamen	18.64%	.0001	**.001**	**patient**	40.54 ± 6.28
				control	34.17 ± 4.96
right pallidum	19.34%	.002	**.010**	**patient**	33.90 ± 5.96
				control	28.41 ± 5.83
right putamen	13.09%	.006	**.015**	**patient**	44.52 ± 6.87
				control	39.37 ± 5.74
Standard technique-mapping					
T1 mapping					
left pallidum	4.37%	.017	.11	**patient**	912.10 ± 44.94
				control	873.92 ± 62.56
right pallidum	3.44%	.047	.22	**patient**	894.75 ± 43.13
				control	864.98 ± 59.04
T2 mapping					
GM	5.88%	.0001	**.001**	**patient**	98.48 ± 5.40
				control	104.27 ± 5.5
right caudate	8.53%	.006	**.042**	**patient**	86.23 ± 7.22
				control	93.59 ± 10.43

Abbreviations: NAWM: normal-appearing white matter; PD, Parkinson's disease; GM: grey matter. Significant P-values after multiple testing corrections are marked in bold. The contralateral structure is used for comparison.

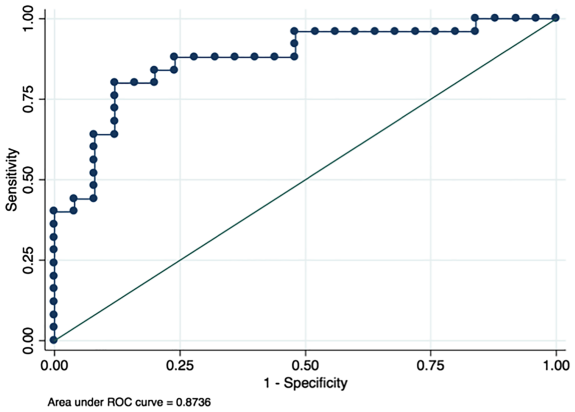

FIGURE 4 Receiver-operating characteristic (ROC) area under the curve (AUC) of patient-control separation based on cortical grey matter and left putaminal T2 relaxation times

Cohen's D = 0.66, CI of D 0.09-1.23), revealing longer T2 relaxation times in PD patients compared with controls. T2 relaxation times differed somewhat in NAWM (P = .070; Cohen's D = 0.58, CI of D 0.02-1.15), while there was no significant difference in cortical GM (68.98 ± 9.90 in PD vs. 66.64 ± 9.28 ms in controls; P = .394). In all ROIs with significant differences between PD patients and controls, mean T2 relaxation time was shorter in controls. Relative differences between significantly differing ROIs were larger than in T1 mapping: 9.09% to 19.34% (Table 1).

An ROI separation depending on the putatively more affected hemisphere (MAH) revealed the putamen of the MAH as a relevant separation factor between PD patients and controls for both T1 and T2 mapping. However, an effect on R^2 was observed only for T1 mapping (R^2 = 0.437), with cortical GM remaining the other influential factor in this two-factor stepwise regression model (GM: OR = 0.945, P = .001; putamen MAH: OR = 1.026, P = .006). In T2 mapping, the putamen of the MAH was identified as the only significant factor separating patients and controls (OR = 1.262, P = .001), but at a lower R^2 of 0.267 compared with a hemispherical comparison of ROIs.

3.3 | Standard ROI-based mapping and differences to MRF

Standard T1 and T2 mapping techniques identified ROIs as significantly differing between PD patients and controls that were different from MRF-based findings. These were fewer, and in the case of T1 mapping, were no longer significant after correcting for a false discovery rate (Table 1). In part, larger standard deviations were the underlying reason in standard mapping, for example, for cortical GM (controls 1482.96 ± 199.73 ms vs. patients 1438.51 ± 66.46 ms, P = .30). The paired t-test analysis also revealed significant differences between relaxation times measured with the standard technique in comparison with MRF-based mapping in many ROIs, and especially with regard to T2 mapping (Table 2). MRF-based T2 mapping generated relaxation times that were about half of those determined with standard mapping in the same structure. However, the correlation of values was still high between many structures, especially with regard to T1 mapping techniques (Table 2).

3.4 | Correlation of relaxation times with clinical parameters

As expected, a priori testing showed a strong correlation between the time since diagnosis and UPDRS (R = +0.60; P = .002). Concerning the analysis of both full groups of patients and controls, relaxation time as measured in the left pallidum by standard T1 mapping correlated negatively with disease duration (R = −0.47, P = .02). Otherwise, none of the ROI-based relaxation times correlated to a significant degree with either UPDRS or disease duration (MRF-based T1 and T2 mapping R = −0.37 to 0.001, P = .12 to .99; standard T1 and T2 mapping R = −0.10 to 0.37, P = .08 to .99).

A subgroup analysis of the lowest quartile of patients by onset (ie, with the most recent onset of symptoms, n = 6, mean onset 2.74 ± 0.80 years before MRI, mean UPDRS 30.20 ± 25.60, mean age 66.71 ± 9.42 years) versus those with the most longstanding diagnosis (n = 6, mean onset 14.87 ± 3.19 years before MRI, mean UPDRS 63.70 ± 23.0, mean age 68.35 ± 6.22 years; both groups differing significantly in UPDRS, P = .0001, and onset duration, P = .001, but not significantly by age) revealed that in all cases MRF-based T1 relaxation times were shorter in PD patients than in controls, but that patients suffering from a significantly longer disease duration (P = .001) and higher UPDRS (P = .037) did not necessarily have significantly shorter relaxation times in any of the ROIs compared with those with a more recent diagnosis. Indeed, only the left putamen differed significantly between the onset-stratified groups (P = .04; longest diagnosis: 1080.51 ± 48.32 ms vs. shortest diagnosis: 1141.94 ± 40.94 ms). Similarly, T2 relaxation times in PD patients were longer in both more recent and longstanding subgroups than in controls. Still, no significant differences between both subgroups could be identified.

TABLE 2 Paired t-test results and Spearman correlation results comparing standard and MRF-based relaxation times

T1 mapping techniques				T2 mapping techniques			
ROI	**2-tailed t-test *P*-value**	**Spearman R**	***P*-value**	**ROI**	**2-tailed t-test *P*-value**	**Spearman R**	***P*-value**
GM	**.0001**	.456	**.001**	GM	**.0001**	.190	.186
NAWM	**.0001**	.898	**.0001**	NAWM	**.0001**	.468	**.001**
left thalamus	**.0001**	.428	**.002**	left thalamus	**.0001**	.163	.259
left caudate	.385	.250	.080	left caudate	**.0001**	.369	**.008**
left putamen	**.0001**	.357	**.011**	left putamen	**.0001**	.281	**.048**
left pallidum	**.0001**	.663	**.0001**	left pallidum	**.0001**	.445	**.001**
left hippocampus	.077	.031	.829	left hippocampus	**.0001**	.070	.630
left amygdala	**.0001**	.036	.802	left amygdala	**.0001**	−.092	.523
right thalamus	**.047**	.318	**.025**	right thalamus	**.0001**	.190	.185
right caudate	**.0001**	.455	**.001**	right caudate	**.0001**	.157	.276
right putamen	.500	.297	**.036**	right putamen	**.0001**	.322	**.023**
right pallidum	**.0001**	.570	**.0001**	right pallidum	**.0001**	.445	**.001**
right hippocampus	.071	.286	**.044**	right hippocampus	**.0001**	.312	**.027**
right amygdala	**.0001**	−.104	.471	right amygdala	**.0001**	.160	.267

Abbreviations: GM, grey matter; NAWM, normal-appearing white matter. Regions of interest (ROIs) with significant differences in relaxation times depending on the mapping technique and significant correlations between relaxation times derived from different methods are marked in bold. Note that values can vary significantly in absolute numbers, but still can correlate strongly.

3.5 | Additional volumetric analyses

After normalisation, PD patients and controls differed volumetrically in both caudate nuclei: left caudate (4.16 ± 0.51 cm^3 in controls vs. 3.71 ± 0.68 cm^3 in PD; $P = .01$) and right caudate (4.20 ± 0.60 cm^3 in controls vs. 3.56 ± 0.79 cm^3 in PD; $P = .02$).

3.6 | Patient comfort survey

Three out of 25 patients rated the MRF programme as unpleasant to undergo, while 16 were indifferent and the remaining six considered the programme as particularly comfortable. Twenty-three out of 25 patients preferred the MRF protocol to the standard hospital MR protocol, mainly because of the potentially shorter scan times.

4 | DISCUSSION

This pilot study revealed that both MRF-based T1 and T2 mapping deliver a relevant discriminatory power to differentiate PD patients from controls. Notably, structures other than the basal ganglia show significant relaxation time differences. PD patients experienced MRF as comfortable. The comparability with standard mapping techniques is, however, very limited, and the exact longitudinal association with neurodegenerative changes and symptoms also remains uncertain.

It should be noted that while the core focus of this study was MRF-based mapping, differences in brain structure volumes were not significant between patients and controls, despite a relative reduction in bilateral patient caudate volume. This corroborates findings by others such as Pitcher et al,[27] who suggested that the reduction in volume is related to the loss of neuronal function in the striatum. This is in agreement with the general comparability between patients and controls in the current study, as substantial atrophy can be a bias in ROI-based studies due to limited voxels and increasing partial volume effects.

PD patients demand short diagnostic MRI protocols. Currently, standard MRI can still be lengthy and, in particular, more established MRI biomarkers for PD are not quantitative. There are conventional T1 or T2 mapping PD studies that mainly found relaxation time differences in brain regions that are particularly susceptible to neurodegeneration in PD.[7,8,28–30] In the current study, we focused on the general detectability of group differences by MRF making use of the global changes that can potentially be observed in PD,[7] and deliberately sacrificed the spatial resolution to analyse classic structures such as the substantia nigra[29] in order to guarantee a good SNR. From one measurement only, MRF provides both T1

and T2 maps, and—although not being the focus of this study—images with different contrast weightings. The time-saving potential and comfort improvement aspects are apparent.

In this exploratory study, MRF-based T1 relaxation times were consistently shorter, while T2 relaxation times were longer in patients than in controls. The T1 shortening identified is consistent with the conventional T1 mapping results of Nurnberger et al,[7] who suggested an increase of the cellular compartment in PD, causing a shift of iron from bound Fe^{3+} towards more soluble Fe^{2+}, which has a stronger T1 shortening effect. In their study, T1 relaxation time differences in PD were only observed in the long-term follow-up scans, whereas initial T1 values were normal.[7] T1 differences in our study, however, were observed in the cortical GM at only one time-point. This might hint at a sensitivity of MRF-based T1 mapping to disease-related changes. In addition, diffuse cortical relaxation time changes strengthen the concept of PD affecting the entire brain rather than only basal ganglia structures.[28] Notably, standard T1 mapping in our study did not reveal GM differences either. While standard T1 mapping in GM also revealed shorter relaxation times in patients, the standard deviations were too large to render significance. By tendency, T1 mapping results based on the standard technique were, however, comparable with MRF-based results in GM, as could be verified by a usually good correlation.

At this point, the surprising result of longer relaxation times observed with standard T1 mapping in the pallidum of patients must be discussed, which is in contrast to the general trend observed in both MRF-based and standard IR T1 mapping in this study, as well as in others.[7] Unfortunately, the literature is sparse regarding mapping in the pallidum of PD patients and MRF-based T1 mapping showed no significant differences between both groups. While a shortening of the T1 relaxation time in PD is more likely to be expected (eg, due to iron deposition), and could be observed in MRF-based mapping as well as in, for example, cortical GM by standard mapping, it is also known that the neurochemical changes in PD are complex.[31] At least one earlier study mapping different PD spectrum subtypes identified variable effects on R1 in the pallidum.[32]

Different to T1 mapping, significant MRF-based T2 relaxation time changes were nearly limited to the basal ganglia in this study and were poorly comparable between MRF-based and standard techniques. Previous studies investigated T2* relaxation times in PD, which are mainly influenced by susceptibility effects. These studies found T2* relaxation times shortening in PD patients in the pallidum and frontal cortices of PD patients, respectively,[8,28] or faster R2* relaxation rates, and hence shorter T2* relaxation times, as well as T2 shortening in the substantia nigra.[30,33] Due to a mutual interference of effects, T2* primarily measures susceptibility effects of the tissue from paramagnetic and ferromagnetic substances, whereas T2 relates to spin–spin effects of the water protons. T2 values thus predominantly reflect the free water content and water proton mobility as well as the cell density and microstructural properties of the tissue under investigation. Still, some comparability between T2* as performed by others and T2 mapping remain, which is reflected in our findings when comparing standard T2 mapping, which showed a focal shortening of relaxation times in the GM of patients compared with controls. The absolute relaxation times reveal a substantial discrepancy between MRF-based and standard technique T2 mapping in this study. The main finding, however, is a differentiation between patients and the control group that is based on more structures using MRF-based T2 mapping, and therefore potentially improved, at equal variance for each of these groups (cf. Table 1). Still, the reasons for the substantial and partially unexpected differences between standard T2 mapping and MRF-based mapping need further exploration. MRF-based T1 relaxation times were, by contrast, relatively consistent with studies using classic mapping techniques.[34]

In some ROIs, relaxation time differences between PD patients and controls were only found unilaterally in one hemisphere. This asymmetry was already observed by Baudrexel et al and was linked to the clinically MAH.[29] We, however, did not observe that relaxation times showed a larger deviation from controls on the clinically MAH than on the less affected side.

Our study could not identify a relationship between relaxation times and UPDRS or disease duration. At the same time, a correlation between UPDRS and disease duration could be established. Similar observations were made for classic T1 mapping in PD patients[29] and the intra-individual longitudinal follow-up study by Nurnberger et al, who uncovered a more rapid intra-individual decrease in T1 relaxation over time in PD patients than in controls, while not being able to link relaxation times to UPDRS either.[7] Consequently, T1 mapping might be a surrogate for disease progression, but not for disease severity measured at one point in time.

Patient acceptance of MRF as a one sequence-based mean of MRI diagnostics was high in this study compared with conventional MRI. MRF can also be used to provide synthetic MR images imitating the contrast of conventional weighted MR sequences. Therefore, this study can be the first leading towards an alternative partial replacement of conventional weighting-based MRI and shortening of patient scan times. This is particularly valuable in helping those patients with motor impairments and other problems such as claustrophobia to lie still in the MRI scanner.

This is a first feasibility study. Considering its limited size, it revealed that MRF can deliver T1 and T2 maps which show robust differences with usually strong, but at least medium effect sizes, albeit that these results have limited comparability with standard mapping techniques.

In the future, MRF for PD patients must retain its capacity to challenge classical MRI biomarkers (eg, through secondary feature analysis), as well as its diagnostic accuracy in early cases of PD or differential diagnostics towards clinically similar conditions. More importantly, imaging biomarkers should demonstrate sensitivity to early forms of disease that are still clinically vague.[29] In the current study, no significant differences were identified between more affected long-term patients and their recently diagnosed counterparts. This may corroborate the findings of others regarding a limited clinical association of relaxometry as a potential imaging biomarker,[7] but is more likely due to the limited size of the subgroups being compared.

As a current limitation, and because of the aforementioned reasons, the MRF sequence applied here needs optimisation regarding resolution. Our focus, therefore, did not include an analysis of very small structures relevant in PD, such as the substantia nigra, which makes this study less comparable.[29,30] Further, it remains an unresolved question as to whether our results are specific for PD or could theoretically be identified in other neurodegenerative conditions. One future clinical focus should be directed towards the differentiation of clinically different subforms of PD to establish a threshold with which to identify early PD. It is important to stress that this is a single-centre study: its results will need to prove reproducibility elsewhere and are subject to the current sequence and postprocessing parameters. For a complete picture, it should be noted that acute pharmacokinetic effects from levodopa medication (eg, on blood flow) could be a compromising cofactor possibly influencing individual mapping results.

In conclusion, MRF is perceived as comfortable by patients and can help to identify PD patients based on T1 and T2 mapping to a substantial degree, but with limited comparability concerning standard mapping techniques. Since this is a first exploration of MRF in PD patients, these results should be confirmed in a larger set of patients with early symptoms.

ACKNOWLEDGEMENTS

The authors thank PD Drs Oliver Kaut and Veronika Purrer, University Hospital Bonn, Neurology Department, for introducing interested patients. Vera Catharina Keil and Stilyana Peteva Bakoeva contributed equally to this study. Open access funding enabled and organized by Projekt DEAL.

ORCID

Vera Catharina Keil https://orcid.org/0000-0001-8699-3506

REFERENCES

1. GBD 2016 Parkinson's Disease Collaborators. Global, regional, and national burden of Parkinson's disease, 1990-2016: a systematic analysis for the Global Burden of Disease Study 2016. *Lancet Neurol*. 2018;17(11):939-953.
2. Weingarten CP, Sundman MH, Hickey P, Chen NK. Neuroimaging of Parkinson's disease: Expanding views. *Neurosci Biobehav Rev*. 2015;59:16-52.
3. Hoehn MM, Yahr MD. Parkinsonism: onset, progression and mortality. *Neurology*. 1967;17(5):427-442.
4. Bajaj N, Hauser RA, Grachev ID. Clinical utility of dopamine transporter single photon emission CT (DaT-SPECT) with (123I) ioflupane in diagnosis of Parkinsonian syndromes. *J Neurol Neurosurg Psychiatry*. 2013;84(11):1288-1295.
5. Politis M. Neuroimaging in Parkinson disease: from research setting to clinical practice. *Nat Rev Neurol*. 2014;10(12):708-722.
6. Lonnfors-Weitzel T, Weitzel T, Slotboom J, et al. T2-relaxometry predicts outcome of DBS in idiopathic Parkinson's disease. *Neuroimage Clin*. 2016;12:832-837.
7. Nurnberger L, Gracien RM, Hok P, et al. Longitudinal changes of cortical microstructure in Parkinson's disease assessed with T1 relaxometry. *Neuroimage Clin*. 2017;13:405-414.
8. Egger K, Amtage F, Yang S, et al. T2* relaxometry in patients with Parkinson's disease: use of an automated atlas-based approach. *Clin Neuroradiol*. 2018;28(1):63-67.
9. Al-Bachari S, Parkes LM, Vidyasagar R, et al. Arterial spin labelling reveals prolonged arterial arrival time in idiopathic Parkinson's disease. *Neuroimage Clin*. 2014;6:1-8.
10. Ma D, Gulani V, Seiberlich N, et al. Magnetic resonance fingerprinting. *Nature*. 2013;495(7440):187-192.
11. Badve C, Yu A, Rogers M, et al. Simultaneous T1 and T2 brain relaxometry in asymptomatic volunteers using magnetic resonance fingerprinting. *Tomography*. 2015;1(2):136-144.
12. Badve C, Yu A, Dastmalchian S, et al. MR fingerprinting of adult brain tumors: initial experience. *Am J Neuroradiol*. 2017;38(3):492-499.
13. Deuschl G. Leitlinien für Diagnostik und Therapie in der Neurologie - Idiopathisches Parkinson-Syndrom. In: AWMF D, ed 2016 (German). https://www.dgn.org/images/red_leitlinien/LL_2016/PDFs_Download/030010_LL_langfassung_ips_2016.pdf Last accessed 1 July 2020.
14. Postuma RB, Berg D, Adler CH, et al. The new definition and diagnostic criteria of Parkinson's disease. *Lancet Neurol*. 2016;15(6):546-548.
15. Rhodius-Meester HFM, Benedictus MR, Wattjes MP, et al. MRI visual ratings of brain atrophy and white matter hyperintensities across the spectrum of cognitive decline are differently affected by age and diagnosis. *Front Aging Neurosci*. 2017;9:117.
16. Jiang K, Zhu Y, Jia S, Wu Y, Liu X, Chung YC. Fast T1 mapping of the brain at high field using Look-Locker and fast imaging. *Magn Reson Imaging*. 2017;36:49-55.
17. Sommer K, Amthor T, Doneva M, Koken P, Meineke J, Bornert P. Towards predicting the encoding capability of MR fingerprinting sequences. *Magn Reson Imaging*. 2017;41:7-14.
18. Hattingen E, Muller A, Jurcoane A, et al. Value of quantitative magnetic resonance imaging T1-relaxometry in predicting contrast-enhancement in glioblastoma patients. *Oncotarget*. 2017;8(32):53542-53551.
19. Keil VC, Bakoeva SP, Jurcoane A, et al. MR fingerprinting as a diagnostic tool in patients with frontotemporal lobe degeneration: A pilot study. *NMR Biomed*. 2019;32(11):e4157.
20. Roemer PB, Edelstein WA, Hayes CE, Souza SP, Mueller OM. The NMR phased array. *Magn Reson Med*. 1990;16(2):192-225.
21. Smith SM, Zhang Y, Jenkinson M, et al. Accurate, robust, and automated longitudinal and cross-sectional brain change analysis. *Neuroimage*. 2002;17(1):479-489.
22. Jenkinson M, Beckmann CF, Behrens TE, Woolrich MW, Smith SM. FSL. *Neuroimage*. 2012;62(2):782-790.
23. Yushkevich PA, Piven J, Hazlett HC, et al. User-guided 3D active contour segmentation of anatomical structures: significantly improved efficiency and reliability. *Neuroimage*. 2006;31(3):1116-1128.
24. Benjamini Y, Hochberg Y. Controlling the false discovery rate - a practical and powerful approach to multiple testing. *J Royal Stat Soc*. 1995;57:289-300.

25. Peduzzi P, Concato J, Feinstein AR, Holford TR. Importance of events per independent variable in proportional hazards regression analysis. II. Accuracy and precision of regression estimates. *J Clin Epidemiol*. 1995;48(12):1503-1510.
26. Babyak MA. What you see may not be what you get: a brief, nontechnical introduction to overfitting in regression-type models. *Psychosom Med*. 2004;66(3):411-421.
27. Pitcher TL, Melzer TR, Macaskill MR, et al. Reduced striatal volumes in Parkinson's disease: a magnetic resonance imaging study. *Transl Neurodegener*. 2012;1(1):17.
28. Mondino F, Filippi P, Magliola U, Duca S. Magnetic resonance relaxometry in Parkinson's disease. *Neurol Sci*. 2002;23(Suppl 2):S87-S88.
29. Baudrexel S, Nurnberger L, Rub U, et al. Quantitative mapping of T1 and T2* discloses nigral and brainstem pathology in early Parkinson's disease. *Neuroimage*. 2010;51(2):512-520.
30. Pyatigorskaya N, Sharman M, Corvol JC, et al. High nigral iron deposition in LRRK2 and Parkin mutation carriers using R2* relaxometry. *Mov Disord*. 2015;30(8):1077-1084.
31. Toulorge D, Schapira AH, Hajj R. Molecular changes in the postmortem parkinsonian brain. *J Neurochem*. 2016;139(Suppl 1):27-58.
32. Focke NK, Helms G, Pantel PM, et al. Differentiation of typical and atypical Parkinson syndromes by quantitative MR imaging. *Am J Neuroradiol*. 2011;32(11):2087-2092.
33. Vymazal J, Righini A, Brooks RA, et al. T1 and T2 in the brain of healthy subjects, patients with Parkinson disease, and patients with multiple system atrophy: relation to iron content. *Radiology*. 1999;211(2):489-495.
34. Kumar R, Delshad S, Woo MA, Macey PM, Harper RM. Age-related regional brain T2-relaxation changes in healthy adults. *J Magn Reson Imaging*. 2012;35(2):300-308.

How to cite this article: Keil VC, Bakoeva SP, Jurcoane A, et al. A pilot study of magnetic resonance fingerprinting in Parkinson's disease. *NMR in Biomedicine*. 2020;33:e4389. https://doi.org/10.1002/nbm.4389